

1
2
3
4
5
6
7
8
9
10
11
12
13
14
15
16
17
18
19
20
21
22
23
24
25
26
27
28
29
30
31

DR. JIAN-SHENG (J-S) YE (Orcid ID : 0000-0001-5335-7896)

DR. MANUEL DELGADO-BAQUERIZO (Orcid ID : 0000-0002-6499-576X)

Article type : Primary Research Articles

Multifunctionality debt in global drylands linked to past biome and climate

Running head: Legacy effects on dryland multifunctionality

Jian-Sheng Ye^{1*}, Manuel Delgado-Baquerizo^{2,3}, Santiago Soliveres⁴ and Fernando T. Maestre³

¹State Key Laboratory of Grassland Agro-ecosystems, School of Life Sciences, Key Laboratory for Semi-Arid Climate Change of the Ministry of Education, Lanzhou University, No. 222, South Tianshui Road, Lanzhou 730000, China

²Cooperative Institute for Research in Environmental Sciences, University of Colorado, Boulder, CO 80309, USA.

³Departamento de Biología y Geología, Física y Química Inorgánica, Escuela Superior de Ciencias Experimentales y Tecnología, Universidad Rey Juan Carlos, Calle Tulipán Sin Número, Móstoles 28933, Spain.

⁴Departamento de Ecología, Universidad de Alicante, 03690 San Vicente del Raspeig (Alicante), Spain.

Correspondence to: J.-S. Y.; telephone, +86 13919145033; email address, yejsh@lzu.edu.cn

Keywords: plant productivity, plant species richness, precipitation, arid climate, last glacial maximum, nutrient stocks, nutrient transformation rates, palaeoclimate

This is the author manuscript accepted for publication and has undergone full peer review but has not been through the copyediting, typesetting, pagination and proofreading process, which may lead to differences between this version and the Version of Record. Please cite this article as [doi: 10.1111/GCB.14631](https://doi.org/10.1111/GCB.14631)

This article is protected by copyright. All rights reserved

32

33 **Paper type:** Primary Research Article **Abstract**

34 Past vegetation and climatic conditions are known to influence current biodiversity
35 patterns. However, whether their legacy effects affect the provision of multiple
36 ecosystem functions, i.e. multifunctionality, remains largely unknown. Here we
37 analyzed soil nutrient stocks and their transformation rates in 236 drylands from six
38 continents to evaluate the associations between current levels of multifunctionality
39 and legacy effects of last glacial maximum (LGM) desert biome distribution and
40 climate. We found that past desert distribution and temperature legacy, defined as
41 increasing temperature from LGM, were negatively correlated with contemporary
42 multifunctionality even after accounting for predictors such as current climate, soil
43 texture, plant species richness and site topography. Ecosystems that have been deserts
44 since the LGM had up to 30% lower contemporary multifunctionality compared with
45 those that were non-deserts during the LGM. In addition, ecosystems that experienced
46 higher warming rates since the LGM had lower contemporary multifunctionality than
47 those suffering lower warming rates, with a ~9% reduction per extra °C. Past desert
48 distribution and temperature legacies had direct negative effects, while temperature
49 legacy also had indirect (via soil sand content) negative effects on multifunctionality.
50 Our results indicate that past biome and climatic conditions have left a strong
51 “functionality debt” in global drylands. They also suggest that ongoing warming and
52 expansion of desert areas may leave a strong fingerprint in the future functioning of
53 dryland ecosystems worldwide that needs to be considered when establishing
54 management actions aiming to combat land degradation and desertification.

55 **1. INTRODUCTION**

56 Ecosystem attributes and functions, such as biodiversity and nutrient cycling, are not
57 only driven by current environmental conditions, but also by those they have
58 experienced in the past. The climate existing thousands of years ago has left a
59 detectable fingerprint in the current distribution of plant and microbial communities
60 (Blonder et al., 2018; Delgado-Baquerizo, Bissett, et al., 2017; Delgado-Baquerizo et
61 al., 2018; Pärtel et al., 2017; Weigelt, Steinbauer, Cabral, & Kreft, 2016). Similarly,
62 changes in land use that occurred centuries ago have been found to affect current soil
63 carbon and nitrogen contents and cycling (Delgado-Baquerizo, Eldridge, et al., 2017;
64 Dupouey, Dambrine, Laffite, & Moares, 2002). Despite the growing evidence of the
65 impacts of past legacies on the contemporary structure and functioning of terrestrial

66 ecosystems, we lack empirical studies aiming to quantify the legacy effects of past
67 climate and biome distribution on the current provision of multiple ecosystem
68 functions (multifunctionality) related to nutrient stocks and their transformation rates.
69 Quantifying these legacy effects is important not only to better understand the factors
70 driving current variation in multifunctionality, but also to help foresee potential
71 limitations in the provision of ecosystem services in the future derived from current
72 rates of land degradation and climate change.

73 Legacy effects of past conditions on multifunctionality can be caused by
74 long-term gains and losses of energy and nutrients accumulated over millennia
75 (Delgado-Baquerizo, Eldridge, et al., 2017; Svenning, Eiserhardt, Normand, Ordonez,
76 & Sandel, 2015). Furthermore, past climate or vegetation have been found to affect
77 current patterns of soil texture and plant traits globally (Blonder et al., 2018; Prentice
78 et al., 1992). Soil texture and plant traits are known to influence ecosystem functions
79 (Blonder et al., 2018; Prentice et al., 1992). For example, loamy soils can carry over
80 moisture from the wet season into the dry season for plant production more effectively
81 than sandy soils (Prentice et al., 1992). Therefore, the legacy of past conditions on
82 multifunctionality can also be indirectly mediated by changes in variables including
83 soil texture (Prentice et al., 1992), plant functional traits (Blonder et al., 2018) and
84 microbial communities (Delgado-Baquerizo, Bissett, et al., 2017). Differentiating
85 between these direct and indirect effects is of crucial importance to better quantify
86 which part of legacy effects can be managed for (i.e., those mediated by biodiversity)
87 from those that cannot be buffered (i.e., the direct effect of past biome and climate
88 conditions).

89 Global drylands, including hyper-arid, arid, semi-arid and dry-subhumid
90 ecosystems, have been projected to experience higher warming rates with ongoing
91 climate change than humid areas (Huang, Yu, Dai, Wei, & Kang, 2017). Increases in
92 aridity due to ongoing global warming will increase the global extent of drylands,
93 which already cover ~45% of the terrestrial surface (Právělie, 2016), by 11-23% by
94 the end of this century (Huang, Yu, Guan, Wang, & Guo, 2016). Such aridification
95 will threaten the livelihoods of people living in these areas, particularly in the
96 developing world, and will exacerbate the risk of land degradation and desertification,
97 which are already negatively affecting 250 million people (Reynolds et al., 2007).

98 Given the inherently slow dynamics of soil nutrient buildup and plant
99 productivity in drylands compared to other ecosystems (Fischer & Turner, 1978;

100 Huang et al., 2017), we would expect strong negative legacy effects of past biome and
101 climate conditions on current multifunctionality levels, i.e. a “functionality debt”. The
102 desert biome is characterized by low vegetation cover, and thus high soil erosion rates
103 and low nutrient contents (Borrelli et al., 2017; Olson et al., 2001; Ray & Adams,
104 2001). Therefore, ecosystems under a desert biome thousands of years ago should
105 have lower multifunctionality than ecosystems under a more mesic biome in the same
106 period, regardless of their current climate and biome. However, the impact of these
107 legacy effects on dryland multifunctionality, as well as whether these effects are
108 biodiversity- and soil texture-dependent, remains to be evaluated. Moreover, the
109 relative importance of functionality debts vs. current climate and biome as drivers of
110 contemporary multifunctionality is largely unknown.

111 To address these gaps in our knowledge, we coupled data from a field survey of
112 236 drylands from six continents (Figure 1) to existing databases on the historical
113 distribution of past biomes and climates (Fick & Hijmans, 2017; Olson et al., 2001;
114 Ray & Adams, 2001) to evaluate the legacy effects of desert distribution and climate
115 during the last glacial maximum (LGM, about 22000 years ago) on current
116 multifunctionality levels. Weigelt et al. (2016) suggested that glacial conditions have
117 been more common than interglacial conditions during recent evolutionary time. The
118 distribution of biomes during the LGM is representative of the dominant
119 environmental conditions (including climate) during this period (Pärtel et al., 2017).
120 Therefore, the LGM biome distribution is likely to have a strong legacy effect on
121 current multifunctionality levels. We hypothesized that areas that have been under the
122 desert biome during LGM should have a reduced contemporary multifunctionality
123 compared to current deserts that were not so during the LGM (i.e. they exhibit a
124 functionality debt). Furthermore, Maestre et al. (2012) found that multifunctionality
125 was reduced with increasing temperature in global drylands. Therefore, we also
126 hypothesized that current drylands that have suffered higher increases in temperature
127 since the LGM will have lower multifunctionality when compared to those that have
128 undergone lower warming rates.

130 **2. MATERIALS AND METHODS**

131 **2.1 Study sites**

132 We used data from a global field survey conducted in 236 dryland ecosystems from
133 19 countries (Figure 1, see also Table S1 in Supporting Information and Data S1). Our

134 field survey was limited by funding, accessibility to locations and geopolitical and
135 safety circumstances. Because of these, a truly global random sampling covering all
136 dryland locations worldwide was not possible. Nevertheless, our sampling aimed to
137 cover a large range of the environmental conditions and soil/vegetation types found in
138 dryland ecosystems worldwide. The 236 studied ecosystems cover a mean annual
139 temperature (MAT) ranging from -1.8 to 28.2 °C, and a mean annual precipitation
140 (MAP) ranging from 66 to 1219 mm. They also cover over 25 categories of soil types
141 from the FAO classification, including all main types present in drylands (Maestre et
142 al., 2012). The vegetation types surveyed include grasslands, shrublands and savannas,
143 and plant species richness varies from 1 to 52 species per 900 m².

144 **2.2 Field survey**

145 We carried out data collection between February 2006 and December 2013 using a
146 standardized sampling protocol. At each site, we surveyed vegetation using four
147 30-m-long transects located parallel and separated 10 m among them (see Maestre et
148 al., 2012 for details). At each transect, we established 20 quadrats of 1.5 m × 1.5 m
149 and used the total number of perennial species found within the 80 quadrats surveyed
150 as our estimation of species richness. We measured slope angle *in situ* with a
151 clinometer. We sampled soils during the dry season in most of the sites using a
152 stratified random procedure. At each plot, we randomly placed five 50 cm × 50 cm
153 quadrats under the canopy of the dominant perennial species and in open areas devoid
154 of perennial vegetation. We collected a composite sample consisting of five 145 cm³
155 soil cores (0 - 7.5 cm depth) from each quadrat, which were bulked and homogenized
156 in the field. When more than one dominant plant species was present, we also
157 collected samples under the canopies of five randomly selected individuals of the
158 co-dominant species. Thus, the number of soil samples varied between 10 and 15 per
159 site. Back in the laboratory, we sieved soil samples using a 2 mm mesh and air-dried
160 them for one month. To facilitate the comparison of results across sites, we shipped
161 the dried soil samples from all sites to Spain (Rey Juan Carlos University) for
162 laboratory analyses.

163 **2.3 Quantifying multifunctionality**

164 To quantify multifunctionality, we selected 12 plant and soil variables that act as
165 surrogates of carbon (C), nitrogen (N) and phosphorus (P) cycling and storage
166 (functions hereafter). Functions related to the C cycle included plant productivity, soil
167 organic C, pentoses and hexoses. Those from N and P cycles included soil nitrate,

168 dissolved organic N, proteins, potential N transformation rate, and enzymatic activity
169 of phosphatase, available inorganic P, total P and inorganic P. These variables are
170 considered to be critical measures of ecosystem functioning in drylands (see Whitford,
171 2002 for a review). We included as many functions as possible while at the same time
172 weighting equally for the three nutrient cycles. The functions selected include “true”
173 ecosystem functions (*sensu* Reiss, Bridle, Montoya, & Woodward, 2009), such as
174 potential N transformation rate, plant productivity and the activity of phosphatase,
175 and nutrient stocks such as soil organic C and total P, which are indicators of nutrient
176 cycling rates over the long term (Manning et al., 2018).

177 We assessed multifunctionality following the averaging approach of Maestre et al.
178 (2012). We averaged the Z scores of the 12 functions to obtain ecosystem
179 multifunctionality. This index is statistically robust (Maestre et al., 2012) and
180 provides a holistic and easily interpretable measure to assess changes in
181 multifunctionality, as the higher the values for the different ecosystem functions we
182 measured, the higher the multifunctionality (Figure S1). We acknowledge that using
183 an *a priori* standardized average may not allow to discriminate when all functions are
184 performing at similar levels from situations when one function could be strongly
185 outperforming the others (Byrnes et al., 2014). However, all individual functions in
186 our dataset positively correlated with multifunctionality, except for soil inorganic P (r
187 = -0.01 , Figure S1). Moreover, we found only two negative correlations between the
188 functions that were of some magnitude ($r = -0.34$ and -0.35), suggesting that there
189 are not strong trade-offs between our surrogates of ecosystem functioning (Table S2).
190 None of the correlations across all 12 functions was higher than 0.6, suggesting that
191 our dataset did not contain high redundancy among the functions studied (Table S2).
192 Multifunctionality calculated from the 12 functions correlated well with that
193 calculated from a dataset of 16 functions ($r = 0.88$, Figure S2), thus it did not vary
194 much when including other functions available, such as soil total nitrogen, amino
195 acids, aromatic compounds or potential nitrogen depolymerisation.

196 We measured soil functions in the laboratory as described in Methods S1 in the
197 Supporting Information. We also measured soil pH with a pH-meter in a 1:2.5
198 (mass:volume, soil:water) suspension, and soil sand content according to Kettler et al.
199 (2001). For all soil variables and functions, we estimated site-level values as the mean
200 values measured in vegetated and open areas, weighted by their respective cover at
201 each site (Maestre et al., 2012). We used the normalized difference vegetation index

202 (NDVI) as a surrogate for plant productivity because it acts as a proxy of
203 photosynthetic activity and large-scale vegetation distribution (Pettoirelli et al., 2005),
204 and it shows good performance vs. other vegetation indices when used in dryland
205 ecosystems such as those we studied (Gaitán et al., 2013). We retrieved NDVI data
206 from the 250-m resolution moderate resolution imaging spectroradiometer (MODIS)
207 aboard NASA's Terra satellites (<http://daac.ornl.gov/index.shtml>). We used the annual
208 integral of NDVI (iNDVI, Ponce Campos et al., 2013) averaged for the period 2000 to
209 2013 as a proxy of plant productivity at our sites. These iNDVI values correlated well
210 with the average NDVI of the images before, during and after each soil and vegetation
211 survey (Pearson's $r = 0.76$, Figure S3). We used the longer term iNDVI as these
212 values are less influenced by short term variations in precipitation and temperature.

213 **2.4 Assessing biome and climatic legacies**

214 We obtained mean annual temperature and precipitation values for each site for both
215 current (1970-2000) and last glacial maximum (LGM; about 22000 years ago)
216 conditions from Worldclim (Fick & Hijmans, 2017). We used the 2.5-minute
217 resolution bioclimatic data for both periods, as 2.5-minute is the highest resolution
218 available for LGM data. We defined climate legacy from LGM as the difference
219 between current and LGM climate values for temperature and precipitation.
220 Temperature and precipitation legacies range from 2.7 °C to 10.7 °C (mean = 4.8 °C,
221 standard deviation = 1.6) and from -300 mm to +600 mm (mean = -14 mm, standard
222 deviation = 114) across sites, respectively.

223 We used the biome maps of Olson et al. (2001) and Ray & Adams (2001) to
224 define current and LGM distributions of desert biomes, respectively (Figure 1), which
225 included both tropical ($\leq 10\%$ vegetation cover) and temperate ($\leq 20\%$ vegetation
226 cover) deserts. The LGM biome map was mainly based on plant fossil data, proxy
227 data sources such as animal and sediment information and palaeoclimatic data (Ray &
228 Adams, 2001). The current biome map is based on the widely recognized global maps
229 of floristic or zoogeographic provinces, global maps of broad vegetation types,
230 consultations from regional experts, and current climatic data (Olson et al., 2001).

231 The current and LGM biome maps include 15 and 24 biomes, respectively.
232 Therefore, we regrouped LGM biomes to match the current classifications according
233 to Pärtel et al. (2017). The desert biome had a larger distribution during LGM than
234 nowadays (Figure 1). Spatially, the distribution of the desert biome largely overlaps
235 with that of arid and hyper-arid regions of the world (Figure 1). However, vegetation

236 distributions were impacted not only by climate (Thomas & Nigam, 2018) but also by
237 changes in sea level, large vertebrate migrations, fire disturbance regimes or
238 geological activity (Olson et al., 2001; Ray & Adams, 2001; Sarnthein, 1978).
239 Therefore, the desert biome is not synonymous with arid and hyper-arid climates
240 (Figure 1).

241 We defined desert legacy as a binary variable depending on whether it was a
242 desert (105 sites) or not (131 sites) during the LGM. Similarly, current desert
243 distribution is a binary variable depending on whether a given site is currently a desert
244 (63 sites) or not (173 sites). We included the two binomial variables in the statistical
245 analyses described below. The desert biomes were delineated based on thresholds of
246 both climate and key ecosystem properties such as vegetation cover (Olson et al.,
247 2001; Ray & Adams, 2001). When key ecosystem properties such as vegetation cover
248 are pushed over given thresholds, ecosystem regime shifts are likely to occur (here
249 from non-desert to desert, D’Odorico, Bhattachan, Davis, Ravi, & Runyan, 2013) and
250 its biodiversity and functions may be greatly altered (Hastings & Wysham, 2010;
251 Pardini, Bueno, Gardner, Prado, & Metzger, 2010). Therefore, the binary variable of
252 desert and non-desert should be a complement to the continuous climatic variables
253 being studied here.

254 **2.5 Statistical analyses**

255 We fitted a generalized least squares (gls) model using multifunctionality as our
256 response variable and desert and climate legacies, current desert and climate, soil pH
257 and sand content, plant species richness, and site elevation and slope as predictors.
258 This approach allows to incorporate in the model a spatial correlation structure to
259 account for the autocorrelation found within our 236 study sites. We evaluated gls
260 models with different spatial correlation structures using the Akaike information
261 criteria (AIC), and found that an exponential spatial correlation structure best
262 described the autocorrelation within the sites surveyed. The gls does not automatically
263 select predictive variables. Therefore, we first included all the potential predictor
264 variables, and then simplified the fitted model using a stepwise variable selection by
265 manually removing at each step the predictor with less explanatory power (Table 1).
266 Finally, we selected the best model with the lowest AIC (Burnham & Anderson, 2003;
267 Shipley, 2009). The semivariogram of the residuals of the final model used suggested
268 that our approach effectively removed spatial autocorrelation (Figure S4). These
269 analyses were carried out with the R package “nlme” version n 3.1-137 (Pinheiro,

270 Bates, DebRoy, Sarkar, & Team, 2012).

271 We then used variation partitioning (Legendre, 2008) based on linear regression
272 to identify the unique portion of variation in multifunctionality explained by four
273 groups of predictors: (1) LGM desert legacy, (2) temperature and precipitation
274 legacies, (3) current temperature, precipitation and desert distribution, and (4) other
275 drivers (location, soil, plant, and site elevation and slope). The variation partitioning
276 approach followed uses partial regression to partition the variance in
277 multifunctionality with respect to the four groups of predictors. Some proportions
278 were attributed to a particular group of predictors (unique variation) and some were
279 shared among all predictors (shared variation). We used adjusted coefficients of
280 determination (R^2) in the variation partitioning to account for the different number of
281 predictors included in each of the four categories. In some cases, the adjusted R^2 can
282 be negative, which means that the predictors explained less variation than expected by
283 chance (Legendre, 2008); we set them to zero. We used permutation tests for
284 redundancy analysis ordination, as described in Oksanen et al. (2018), to test the
285 significance of unique variation explained by each group; the significance of the
286 shared variation was not testable. We conducted variation partitioning analyses using
287 the R package “Vegan” version 2.4-5 (Oksanen et al., 2018).

288 We used confirmatory path analysis (CPA) to further investigate the direct and
289 indirect (via plant species richness and soil properties) effects of current and LGM
290 climates and desert distributions on the multifunctionality of the 236 drylands studied.
291 CPA allows the analysis of multiple variables that can present complex dependencies
292 among them, which enabled us to partition the direct and indirect effects of different
293 predictors (Shipley, 2009). We developed an *a priori* CPA model (Figure S5) that
294 included all the relationships based on previous knowledge of the potential
295 relationships between our variables (Delgado-Baquerizo, Bissett, et al., 2017;
296 Soliveres et al., 2014). We included in the CPA generalized least squares (gls) fitting
297 of multifunctionality, plant/soil variables and their predictor variables (Figure S5). We
298 then simplified the CPA by removing non-significant paths and selected the best
299 model as that having the lowest AIC. The final CPA included a gls fitting using
300 multifunctionality as response variable and the desert and temperature legacies,
301 current temperature, soil sand content, and elevation as predictors, and a second gls
302 fitting using soil sand content as response variable and the temperature legacy, current
303 temperature and precipitation, and as predictors. Since we included the spatial

304 correlation structure within all gls included in the model, CPA also effectively
305 removed the potential autocorrelation among our sites (Figure S6). We conducted
306 CPA using the R package “piecewiseSEM” version 2.0.2 (Lefcheck, 2016).

307 We checked the normality of all variables before and after log- and square-root
308 transformations using the Shapiro-Wilk test as implemented in R, version 3.5.1 (Team,
309 2018). We then selected the transformation that allowed a best fit to a normal
310 distribution for each variable. To address the quadratic relationships observed
311 between multifunctionality and both soil pH and site elevation (Figure S7), we
312 included x and x^2 terms in all statistical analyses, where x is either pH or elevation.
313 We selected the quadratic model over the linear one if the Δ of differences in AIC
314 between these two models, i.e. $AIC_{linear} - AIC_{quadratic}$, was larger than two
315 (Burnham & Anderson, 2003).

316 As recommended (Byrnes et al., 2014; Manning et al., 2018), and to help
317 interpreting our results, we also repeated CPA analyses for all 12 measured functions
318 separately to test whether the effects of climate and biome legacies were consistent on
319 the overall multifunctionality and individual functions (Table 2). Moreover, we
320 conducted CPA for rate- and stock-based multifunctionality, respectively, to test
321 whether the legacy effects were consistent between nutrient stocks and their
322 transformation rates.

323 Plant functional diversity is a major driver of dryland multifunctionality (Gross et
324 al., 2017) that is also likely to be affected by past climate and biome distribution
325 (Blonder et al., 2018). Hence, we also retrieved trait data for two key traits, plant
326 height and specific leaf area, from the TRY database (Kattge et al., 2011) as described
327 in Gross et al. (2017). A total of 123 of the 236 sites surveyed had trait information
328 available (Gross et al., 2017). We also conducted a CPA using these 123 sites to
329 control for potential indirect effects of past conditions on current multifunctionality
330 driven by functional traits. Including trait predictors did not essentially affect our
331 results (Figure S8). However, among the 123 sites with trait information only fifteen
332 are desert biome currently. Such small sample sizes decreased our confidence when
333 testing the hypothesis of functionality debt caused by desert legacies. Therefore, we
334 only present the results using all 236 sites in the main text. We also controlled for
335 regional differences in other potential confounding factors such as human influence
336 (i.e., population pressure and land use; Last of the Wild Data, 2005), by using the
337 residuals after fitting multifunctionality vs. human influence index (Figure S9).

339 3. RESULTS

340 We found a significant negative association between desert legacy and current
341 ecosystem multifunctionality. The mean multifunctionality was 30% ($\pm 6\%$) lower in
342 drylands that were deserts during LGM than those were not (Table 1). Temperature
343 legacy was also negatively and significantly associated with multifunctionality; this
344 variable was reduced by $\sim 9\%$ per degree warming (Table 1). In other words,
345 regardless of their past biome distribution, locations with the largest increases in
346 temperature over the last 22K years had the lowest multifunctionality. Similarly,
347 current temperature was also negatively and significantly associated with
348 multifunctionality, albeit the rate of decrease ($\sim 2\%$ lower per degree warming) was
349 much lower than that observed with temperature legacy (Table 1). Soil sand content
350 was negatively related to multifunctionality (Table 1).

351 Both desert and climate legacies explained unique and significant proportions of
352 variation in multifunctionality (13% in total, Figure 2). Interestingly, current climates
353 and desert distribution explained a small ($< 3\%$), albeit statistically significant ($P <$
354 0.01), unique proportion of variation. Additional environmental predictors including
355 soil, geographical, and plant variables explained the highest unique proportion of
356 variation in multifunctionality ($\sim 33\%$). The shared variation among all predictors was
357 around 2% (Figure 2).

358 Our confirmatory path analysis explained $\sim 43\%$ of the variation in
359 multifunctionality (Figure 3a). It confirmed the strong negative associations between
360 contemporary multifunctionality and past desert distribution and temperatures, even
361 after considering major drivers of dryland multifunctionality such as current climate,
362 soil properties, site topography, plant species richness, functional diversity and human
363 influence (Figures 3 and S8-9). These negative associations were driven by the effects
364 found both on nutrient stocks, such as soil organic carbon, and their transformation
365 rates, such as plant productivity (Table 2), indicating that both were equally sensitive
366 to legacy effects. The negative effects of desert and temperature legacies were also
367 consistent for 60% of the individual functions (vs. only 13% positive effects, Table 2),
368 and when including more functions in our analyses (16 instead of 12 functions, Figure
369 S10). We found that LGM desert and temperature legacies had strong negative direct
370 effects on multifunctionality, which were about 250% stronger than those found for
371 current climate and desert distribution (Figure 3a). Temperature legacies also had

372 indirect (via positive effect on soil sand content) negative effects on multifunctionality
373 (Figure 3a). Desert and climate legacies had a ~ 10% larger standardized total effect
374 (i.e. sum of indirect and direct effects) on multifunctionality than current desert and
375 climate (Figure 3b).

376 Current temperature had both direct and indirect (via soil sand content) negative
377 effects on multifunctionality (Figure 3a). It also had negative effects on about 70% of
378 the individual functions (Table 2). Current precipitation positively and indirectly
379 influenced multifunctionality through the effects on soil sand content, albeit its effects
380 were only about 25% of the respective effect size of desert and temperature legacies
381 (Figure 3b). Soil sand content negatively impacted multifunctionality (Figure 3a); it
382 also had negative effects on seven individual functions (vs. only one positive effect,
383 Table 2). Biodiversity had no significant effects on overall multifunctionality,
384 although it significantly and positively impacted soil organic C, soil hexoses and soil
385 enzymatic activity of phosphatase (Table 2). However, when multifunctionality was
386 calculated based on a different set of functions (16 stocks and rates, Figure S10), we
387 found a positive effect of species richness on multifunctionality.

388

389 **4. DISCUSSION**

390 Our work provides empirical evidence of a long-term functionality debt in global
391 drylands promoted by legacy effects of past temperature and desert biome distribution.
392 These results add to the increasing evidence that past conditions largely influence
393 current ecosystem structure and functioning (Delgado-Baquerizo, Eldridge, et al.,
394 2017; Monger et al., 2015; Ogle et al., 2015; Pärtel et al., 2017), and provide novel
395 insights about the potential impacts of the climatic changes occurring today for future
396 ecosystem functioning. Importantly, here we found that the negative association
397 between legacy effects and multifunctionality was not only related to stocks but also
398 to nutrient transformation rates, which are fundamental components of ecosystem
399 functioning. Moreover, past legacies had always larger effects on multifunctionality
400 than those of current biomes and climate, which cautions about the potential
401 underestimation of the functional consequences of current warming rates, as the total
402 effects may take some time to manifest. Climatic legacy effects were mainly driven
403 by increases in temperature rather than by changes in rainfall, suggesting that ongoing
404 global warming may have a more detrimental effect on the future of dryland
405 multifunctionality than forecasted changes in rainfall patterns.

406 There are several mechanisms explaining the legacy effects of past biome and
407 climate on both stock- and rate-based functions. First, past climate is known to have
408 an effect on soil texture (our results, Prentice et al., 1992) and also on current
409 microbial diversity and plant functional traits patterns (Blonder et al., 2018;
410 Delgado-Baquerizo, Bissett, et al., 2017), which are important factors influencing
411 nutrient flux rates and primary productivity in drylands (Delgado-Baquerizo et al.,
412 2016; Gross et al., 2017). Second, past climate and biome distribution may drive
413 biotic inputs on soils for millennia, something likely to have a substantial influence on
414 current nutrient stocks. This has been previously observed for soil C
415 (Delgado-Baquerizo, Eldridge, et al., 2017) and we found similar results for both N
416 and P stocks. Third, nutrient stocks and their transformation rates are interdependent.
417 The rates of nutrient fluxes are affected not only by current environmental factors
418 such as climate and vegetation type, but also the size of nutrient stocks (Shen,
419 Jenerette, Hui, & Scott, 2016). For example, many ecosystems in drylands are N
420 limited, and thus their rate of primary productivity are influenced by soil N stocks
421 (Harpole, Potts, & Suding, 2007). Nitrogen transformation rate is positively affected
422 by the size of microbial biomass (Chen et al., 2017), which is generally C limited
423 (Conant et al., 2011); therefore, N transformation rate is likely to be positively
424 affected by soil C and N stocks, as already observed in our database
425 (Delgado-Baquerizo et al., 2013). Therefore, changes in nutrient stocks caused by past
426 climate and biome conditions are likely to affect current nutrient transformation rates
427 (see Table 2). In addition to the potential mechanisms behind the legacy effects of
428 past climate, desert biomes are characterized by low vegetation cover and productivity,
429 high soil erosion rates, extremely slow rates of soil formation, reduced nutrient
430 turnover and slow recovery after disturbances (Borrelli et al., 2017; Chandler, Day,
431 Madsen, & Belnap, 2019; Webb, 2002). These characteristics might contribute to the
432 negative legacy effects from past desert distribution observed in our study. It has been
433 estimated that the recovery of ecosystem functioning after anthropogenic disturbances
434 may take from centuries to millenia in drylands (Belnap & Warren, 2002; Lovich &
435 Bainbridge, 1999). Although these examples show legacy effects from relatively
436 shorter timescales compared to that found in our study, they illustrate the inherent
437 slow dynamics in ecosystem functioning typically observed in drylands, and may
438 suggest similar slow recovery after natural disturbances such as climate variation and
439 biome migration.

440 Our findings indicate that a reversal from desert to more mesic biomes may still
441 be impacted by a functionality debt from its past condition. Recovering a disturbed
442 ecosystem might take from centuries to thousands of years, and an interim recovery
443 debt (the reduction of ecosystem functions occurring during ecosystem recovery after
444 disturbance) will accumulate even if complete recovery is reached (Moreno-Mateos et
445 al., 2017). A recent meta-analysis has shown that ecosystems recovering from
446 anthropogenic disturbances such as agricultural transformation and mining had over
447 35% lower C and N stocks compared with “undisturbed” reference areas
448 (Moreno-Mateos et al., 2017). Our results show a “functionality debt” (~30% decline
449 in multifunctionality) of previous environmental conditions associated to desertified
450 drylands, i.e. high aridity and low vegetation cover. Although they are based on past
451 climate and biome distribution, and thus may not necessarily extrapolate into the
452 future, they suggest that the rate of land restoration should consider this functionality
453 debt and exceed that of land degradation by a similar amount to achieve zero net land
454 degradation aimed by international initiatives such as the UNCCD (UNCCD, 2012).

455 Warming reduces soil moisture, and thus inhibits microbial activity, nutrient
456 cycling, plant growth and vegetation cover in drylands (Foley, Costa, Delire,
457 Ramankutty, & Snyder, 2003; Huang et al., 2017; Yin, Roderick, Leech, Sun, &
458 Huang, 2014). Reduction in vegetation cover also increases soil erosion (Casermeiro
459 et al., 2004; Wei et al., 2007), affecting soil texture and thus promoting soil-mediated
460 temperature legacy effects. Therefore, sites experiencing higher warming rates from
461 LGM to current climate have lower multifunctionality than those suffering lower
462 warming rates (Figure 3). Huang et al. (2017; 2016) predicted deleterious effects of
463 ongoing global warming on the world’s drylands, including long-lasting droughts and
464 reduced crop yields and carbon sequestration in the future. In a similar direction, our
465 results provide empirical evidence that a warming from past to today is negatively
466 associated with multiple functions in dryland ecosystems worldwide.

467 Together, our study provides novel evidence that past desert and temperature
468 legacies have detectable imprints on the current multifunctionality of global drylands.
469 They highlight the importance of looking not only at current but past conditions to
470 fully understand current multifunctionality patterns in these ecosystems. Our results
471 also suggest that ongoing climate change, which will increase the expansion of desert
472 areas, might substantially compromise the multifunctionality of global drylands in the
473 future, and that the rate of land restoration should exceed that of land degradation by

474 around one third if we aim to maintain the ecosystem functions that underpin the
475 provision of key services for the 38% of human population in a warmer, and more
476 arid, world.

477

478 **ACKNOWLEDGEMENTS**

479 J.-S.Y. is supported by China Scholarship Council and the National Natural Science
480 Foundation of China (31570467). MDB acknowledges support from the Marie
481 Skłodowska-Curie Actions of the Horizon 2020 Framework Programme
482 H2020-MSCA-IF-2016 under REA grant agreement n° 702057. SS is supported by
483 the Spanish Government under a Ramón y Cajal contract (RYC-2016-20604). This
484 research is supported by the European Research Council (ERC Grant Agreements
485 242658 [BIOCOM] and 647038 [BIODESERT]).

486

487 **REFERENCES**

488 Belnap, J., & Warren, S. D. (2002). Patton's Tracks in the Mojave Desert, USA: An
489 Ecological Legacy. *Arid Land Research and Management*, 16(3), 245-258.
490 doi:<https://doi.org/10.1080/153249802760284793>

491 Blonder, B., Enquist, B. J., Graae, B. J., Kattge, J., Maitner, B. S., Morueta-Holme,
492 N., . . . Violle, C. (2018). Late Quaternary climate legacies in contemporary
493 plant functional composition. *Global Change Biology*, 24(10), 4827-4840.
494 doi:[doi:10.1111/gcb.14375](https://doi.org/10.1111/gcb.14375)

495 Borrelli, P., Robinson, D. A., Fleischer, L. R., Lugato, E., Ballabio, C., Alewell,
496 C., . . . Panagos, P. (2017). An assessment of the global impact of 21st century
497 land use change on soil erosion. *Nature Communications*, 8(1), 2013.
498 doi:[10.1038/s41467-017-02142-7](https://doi.org/10.1038/s41467-017-02142-7)

499 Burnham, K. P., & Anderson, D. R. (2003). *Model selection and multimodel inference:
500 a practical information-theoretic approach*: Springer Science & Business
501 Media.

502 Byrnes, J. E. K., Gamfeldt, L., Isbell, F., Lefcheck, J. S., Griffin, J. N., Hector, A., . . .
503 Emmett, D. J. (2014). Investigating the relationship between biodiversity and
504 ecosystem multifunctionality: challenges and solutions. *Methods in Ecology
505 and Evolution*, 5(2), 111-124. doi:<https://doi.org/10.1111/2041-210X.12143>

506 Casermeiro, M. A., Molina, J. A., de la Cruz Caravaca, M. T., Hernando Costa, J.,
507 Hernando Massanet, M. I., & Moreno, P. S. (2004). Influence of scrubs on

508 runoff and sediment loss in soils of Mediterranean climate. *CATENA*, 57(1),
509 91-107. doi:[https://doi.org/10.1016/S0341-8162\(03\)00160-7](https://doi.org/10.1016/S0341-8162(03)00160-7)

510 Chandler, D. G., Day, N., Madsen, M. D., & Belnap, J. (2019). Amendments fail to
511 hasten biocrust recovery or soil stability at a disturbed dryland sandy site.
512 *Restoration Ecology*, 0(0). doi:[doi:10.1111/rec.12870](https://doi.org/10.1111/rec.12870)

513 Chen, J., Xiao, G., Kuzyakov, Y., Jenerette, G. D., Ma, Y., Liu, W., . . . Shen, W.
514 (2017). Soil nitrogen transformation responses to seasonal precipitation
515 changes are regulated by changes in functional microbial abundance in a
516 subtropical forest. *Biogeosciences*, 14(9), 2513-2525.
517 doi:<https://doi.org/10.5194/bg-14-2513-2017>

518 Conant, R. T., Ryan, M. G., Ågren, G. I., Birge, H. E., Davidson, E. A., Eliasson, P.
519 E., . . . Hopkins, F. M. (2011). Temperature and soil organic matter
520 decomposition rates—synthesis of current knowledge and a way forward.
521 *Global Change Biology*, 17(11), 3392-3404.

522 D’Odorico, P., Bhattachan, A., Davis, K. F., Ravi, S., & Runyan, C. W. (2013).
523 Global desertification: Drivers and feedbacks. *Advances in Water Resources*,
524 51, 326-344. doi:<https://doi.org/10.1016/j.advwatres.2012.01.013>

525 Delgado-Baquerizo, M., Bissett, A., Eldridge, D. J., Maestre, F. T., He, J.-Z., Wang,
526 J.-T., . . . Fierer, N. (2017). Palaeoclimate explains a unique proportion of the
527 global variation in soil bacterial communities. *Nature Ecology & Evolution*,
528 1(9), 1339-1347. doi:<https://doi.org/10.1038/s41559-017-0259-7>

529 Delgado-Baquerizo, M., Eldridge, D. J., Maestre, F. T., Karunaratne, S. B., Trivedi, P.,
530 Reich, P. B., & Singh, B. K. (2017). Climate legacies drive global soil carbon
531 stocks in terrestrial ecosystems. *Science Advances*, 3(4).
532 doi:<https://doi.org/10.1126/sciadv.1602008>

533 Delgado-Baquerizo, M., Eldridge, D. J., Travers, S. K., Val, J., Oliver, I., & Bissett, A.
534 (2018). Effects of climate legacies on above- and belowground community
535 assembly. *Global Change Biology*, in press. doi:[doi:10.1111/gcb.14306](https://doi.org/10.1111/gcb.14306)

536 Delgado-Baquerizo, M., Maestre, F. T., Gallardo, A., Bowker, M. A., Wallenstein, M.
537 D., Quero, J. L., . . . Zaady, E. (2013). Decoupling of soil nutrient cycles as a
538 function of aridity in global drylands. *Nature*, 502, 672.
539 doi:[10.1038/nature12670](https://doi.org/10.1038/nature12670)

540 Delgado-Baquerizo, M., Maestre, F. T., Reich, P. B., Jeffries, T. C., Gaitan, J. J.,
541 Encinar, D., . . . Singh, B. K. (2016). Microbial diversity drives

542 multifunctionality in terrestrial ecosystems. *Nature Communications*, 7, 10541.
543 doi:10.1038/ncomms10541
544 <https://www.nature.com/articles/ncomms10541#supplementary-information>
545 Dupouey, J. L., Dambrine, E., Laffite, J. D., & Moares, C. (2002). Irreversible Impact
546 of past Land Use on Forest Soils and Biodiversity. *Ecology*, 83(11),
547 2978-2984. doi:<https://doi.org/10.2307/3071833>
548 Fick, S. E., & Hijmans, R. J. (2017). WorldClim 2: new 1-km spatial resolution
549 climate surfaces for global land areas. *International Journal of Climatology*,
550 37(12), 4302-4315. doi:<https://doi.org/doi:10.1002/joc.5086>
551 Fischer, R. A., & Turner, N. C. (1978). Plant Productivity in the Arid and Semiarid
552 Zones. *Annual Review of Plant Physiology*, 29(1), 277-317.
553 doi:<https://doi.org/10.1146/annurev.pp.29.060178.001425>
554 Foley, J. A., Costa, M. H., Delire, C., Ramankutty, N., & Snyder, P. (2003). Green
555 Surprise? How Terrestrial Ecosystems Could Affect Earth's Climate. *Frontiers*
556 *in Ecology and the Environment*, 1(1), 38-44.
557 doi:<https://doi.org/10.2307/3867963>
558 Gaitán, J. J., Bran, D., Oliva, G., Ciari, G., Nakamatsu, V., Salomone, J., . . . Maestre,
559 F. T. (2013). Evaluating the performance of multiple remote sensing indices to
560 predict the spatial variability of ecosystem structure and functioning in
561 Patagonian steppes. *Ecological Indicators*, 34, 181-191.
562 doi:<https://doi.org/10.1016/j.ecolind.2013.05.007>
563 Grace, J. B. (2006). *Structural equation modeling and natural systems*. Cambridge,
564 UK: Cambridge University Press.
565 Gross, N., Bagousse-Pinguet, Y. L., Liancourt, P., Berdugo, M., Gotelli, N. J., &
566 Maestre, F. T. (2017). Functional trait diversity maximizes ecosystem
567 multifunctionality. *Nature Ecology & Evolution*, 1, 0132.
568 doi:<https://doi.org/10.1038/s41559-017-0132>
569 Harpole, W. S., Potts, D. L., & Suding, K. N. (2007). Ecosystem responses to water
570 and nitrogen amendment in a California grassland. *Global Change Biology*,
571 13(11), 2341-2348.
572 Hastings, A., & Wysham, D. B. (2010). Regime shifts in ecological systems can occur
573 with no warning. *Ecology Letters*, 13(4), 464-472.
574 doi:<https://doi.org/10.1111/j.1461-0248.2010.01439.x>
575 Huang, J., Yu, H., Dai, A., Wei, Y., & Kang, L. (2017). Drylands face potential threat

576 under 2 °C global warming target. *Nature Climate Change*, 7, 417.
577 doi:<https://doi.org/10.1038/nclimate3275>

578 Huang, J., Yu, H., Guan, X., Wang, G., & Guo, R. (2016). Accelerated dryland
579 expansion under climate change. *Nature Climate Change*, 6, 166–171.
580 doi:[10.1038/nclimate2837](https://doi.org/10.1038/nclimate2837)
581 <https://www.nature.com/articles/nclimate2837#supplementary-information>

582 Kattge, J., DIAZ, S., LAVOREL, S., PRENTICE, I. C., LEADLEY, P., BÖNISCH,
583 G., . . . WIRTH, C. (2011). TRY – a global database of plant traits. *Global
584 Change Biology*, 17(9), 2905-2935.
585 doi:<https://doi.org/10.1111/j.1365-2486.2011.02451.x>

586 Kettler, T. A., Doran, J. W., & Gilbert, T. L. (2001). Simplified method for soil
587 particle-size determination to accompany soil-quality analyses. *Soil Science
588 Society of America Journal*, 65(3), 849-852.
589 doi:<https://doi.org/10.2136/sssaj2001.653849x>

590 Last of the Wild Data. (2005). *Wildlife Conservation Society - WCS, Center for
591 International Earth Science Information Network - CIESIN - Columbia
592 University, Last of the Wild Project, Version 2, 2005 (LWP-2): Global Human
593 Influence Index (HII) Dataset (Geographic)*. Palisades, NY: NASA
594 Socioeconomic Data and Applications Center (SEDAC).

595 Lefcheck, J. S. (2016). piecewiseSEM: Piecewise structural equation modelling in R
596 for ecology, evolution, and systematics. *Methods in Ecology and Evolution*,
597 7(5), 573-579.

598 Legendre, P. (2008). Studying beta diversity: ecological variation partitioning by
599 multiple regression and canonical analysis. *Journal of Plant Ecology*, 1(1), 3-8.
600 doi:<https://doi.org/10.1093/jpe/rtm001>

601 Lovich, J. E., & Bainbridge, D. (1999). Anthropogenic Degradation of the Southern
602 California Desert Ecosystem and Prospects for Natural Recovery and
603 Restoration. *Environmental Management*, 24(3), 309-326.
604 doi:<https://doi.org/10.1007/s002679900235>

605 Maestre, F. T., Quero, J. L., Gotelli, N. J., Escudero, A., Ochoa, V.,
606 Delgado-Baquerizo, M., . . . Zaady, E. (2012). Plant Species Richness and
607 Ecosystem Multifunctionality in Global Drylands. *Science*, 335(6065),
608 214-218. doi:<https://doi.org/10.1126/science.1215442>

609 Manning, P., van der Plas, F., Soliveres, S., Allan, E., Maestre, F. T., Mace, G., . . .

610 Fischer, M. (2018). Redefining ecosystem multifunctionality. *Nature Ecology*
611 *& Evolution*, 2(3), 427-436. doi:<https://doi.org/10.1038/s41559-017-0461-7>

612 Monger, C., Sala, O. E., Duniway, M. C., Goldfus, H., Meir, I. A., Poch, R. M., . . .
613 Vivoni, E. R. (2015). Legacy effects in linked ecological–soil–geomorphic
614 systems of drylands. *Frontiers in Ecology and the Environment*, 13(1), 13-19.
615 doi:<https://doi.org/10.1890/140269>

616 Moreno-Mateos, D., Barbier, E. B., Jones, P. C., Jones, H. P., Aronson, J.,
617 López-López, J. A., . . . Rey Benayas, J. M. (2017). Anthropogenic ecosystem
618 disturbance and the recovery debt. *Nature Communications*, 8, 14163.
619 doi:<https://doi.org/10.1038/ncomms14163>

620 Ogle, K., Barber, J. J., Barron-Gafford, G. A., Bentley, L. P., Young, J. M., Huxman,
621 T. E., . . . Tissue, D. T. (2015). Quantifying ecological memory in plant and
622 ecosystem processes. *Ecology Letters*, 18(3), 221-235.
623 doi:<https://doi.org/10.1111/ele.12399>

624 Oksanen, J., Blanchet, F. G., Friendly, M., Kindt, R., Legendre, P., McGlenn, D., . . .
625 Wagner, H. (2018). *Community Ecology Package. R package v. 2.4-6*.

626 Olson, D. M., Dinerstein, E., Wikramanayake, E. D., Burgess, N. D., Powell, G. V. N.,
627 Underwood, E. C., . . . Kassem, K. R. (2001). Terrestrial Ecoregions of the
628 World: A New Map of Life on Earth. *BioScience*, 51(11), 933-938.
629 doi:[https://doi.org/10.1641/0006-3568\(2001\)051\[0933:teotwa\]2.0.co;2](https://doi.org/10.1641/0006-3568(2001)051[0933:teotwa]2.0.co;2)

630 Pärtel, M., Öpik, M., Moora, M., Tedersoo, L., Szava-Kovats, R., Rosendahl, S., . . .
631 Zobel, M. (2017). Historical biome distribution and recent human disturbance
632 shape the diversity of arbuscular mycorrhizal fungi. *New Phytologist*, 216(1),
633 227-238. doi:<https://doi.org/10.1111/nph.14695>

634 Pardini, R., Bueno, A. d. A., Gardner, T. A., Prado, P. I., & Metzger, J. P. (2010).
635 Beyond the Fragmentation Threshold Hypothesis: Regime Shifts in
636 Biodiversity Across Fragmented Landscapes. *PLOS ONE*, 5(10), e13666.
637 doi:<https://doi.org/10.1371/journal.pone.0013666>

638 Pettorelli, N., Vik, J. O., Myrsetrud, A., Gaillard, J.-M., Tucker, C. J., & Stenseth, N.
639 C. (2005). Using the satellite-derived NDVI to assess ecological responses to
640 environmental change. *Trends in Ecology & Evolution*, 20(9), 503-510.
641 doi:<https://doi.org/10.1016/j.tree.2005.05.011>

642 Pinheiro, J., Bates, D., DebRoy, S., Sarkar, D., & Team, R. C. (2012). nlme: Linear
643 and nonlinear mixed effects models. *R package version*, 3(0).

-
- 644 Ponce Campos, G. E., Moran, M. S., Huete, A., Zhang, Y., Bresloff, C., Huxman, T.
645 E., . . . Starks, P. J. (2013). Ecosystem resilience despite large-scale altered
646 hydroclimatic conditions. *Nature*, *494*(7437), 349-352.
647 doi:<https://doi.org/10.1038/nature11836>
- 648 Právělie, R. (2016). Drylands extent and environmental issues. A global approach.
649 *Earth-Science Reviews*, *161*, 259-278.
650 doi:<https://doi.org/10.1016/j.earscirev.2016.08.003>
- 651 Prentice, I. C., Cramer, W., Harrison, S. P., Leemans, R., Monserud, R. A., &
652 Solomon, A. M. (1992). Special Paper: A Global Biome Model Based on Plant
653 Physiology and Dominance, Soil Properties and Climate. *Journal of*
654 *Biogeography*, *19*(2), 117-134. doi:<https://doi.org/10.2307/2845499>
- 655 Ray, N., & Adams, J. (2001). A GIS-based vegetation map of the world at the Last
656 Glacial Maximum (25,000-15,000 BP). *Internet Archaeology*, *11*.
657 doi:<https://doi.org/10.11141/ia.11.2>
- 658 Reiss, J., Bridle, J. R., Montoya, J. M., & Woodward, G. (2009). Emerging horizons
659 in biodiversity and ecosystem functioning research. *Trends in Ecology &*
660 *Evolution*, *24*(9), 505-514. doi:<https://doi.org/10.1016/j.tree.2009.03.018>
- 661 Reynolds, J. F., Smith, D. M. S., Lambin, E. F., Turner, B. L., Mortimore, M.,
662 Batterbury, S. P. J., . . . Walker, B. (2007). Global Desertification: Building a
663 Science for Dryland Development. *Science*, *316*(5826), 847-851.
664 doi:<https://doi.org/10.1126/science.1131634>
- 665 Sarnthein, M. (1978). Sand deserts during glacial maximum and climatic optimum.
666 *Nature*, *272*, 43. doi:<https://doi.org/10.1038/272043a0>
- 667 Shen, W., Jenerette, D. G., Hui, D., & Scott, L. R. (2016). Precipitation legacy effects
668 on dryland ecosystem carbon fluxes: Direction, magnitude and
669 biogeochemical carryovers. *12*, 9613-9650.
670 doi:<https://doi.org/10.5194/bgd-12-9613-2015>
- 671 Shipley, B. (2009). Confirmatory path analysis in a generalized multilevel context.
672 *Ecology*, *90*(2), 363-368. doi:[doi:doi:10.1890/08-1034.1](https://doi.org/10.1890/08-1034.1)
- 673 Soliveres, S., Maestre, F. T., Eldridge, D. J., Delgado-Baquerizo, M., Quero, J. L.,
674 Bowker, M. A., & Gallardo, A. (2014). Plant diversity and ecosystem
675 multifunctionality peak at intermediate levels of woody cover in global
676 drylands. *Global Ecology and Biogeography*, *23*(12), 1408-1416.
677 doi:<https://doi.org/10.1111/geb.12215>

-
- 678 Svenning, J.-C., Eiserhardt, W. L., Normand, S., Ordonez, A., & Sandel, B. (2015).
679 The Influence of Paleoclimate on Present-Day Patterns in Biodiversity and
680 Ecosystems. *Annual Review of Ecology, Evolution, and Systematics*, 46(1),
681 551-572. doi:<https://doi.org/10.1146/annurev-ecolsys-112414-054314>
- 682 Team, R. C. (2018). R: A Language and Environment for Statistical Computing, R
683 Foundation for Statistical Computing, Austria, 2015. In: ISBN 3-900051-07-0:
684 URL <http://www.R-project.org>.
- 685 Thomas, N., & Nigam, S. (2018). Twentieth-Century Climate Change over Africa:
686 Seasonal Hydroclimate Trends and Sahara Desert Expansion. *Journal of*
687 *Climate*, 31(9), 3349-3370. doi:<https://doi.org/10.1175/jcli-d-17-0187.1>
- 688 Trabucco, A., & Zomer, R. J. (2009). *Global Aridity Index (Global-Aridity) and*
689 *Global Potential Evapo-Transpiration (Global-PET) Geospatial Database.*
690 *CGIAR Consortium for Spatial Information. Published online, available from*
691 *the CGIAR-CSI GeoPortal at: <http://www.csi.cgiar.org>.* Retrieved from:
692 <http://www.csi.cgiar.org>
- 693 UNCCD. (2012). Zero Net Land Degradation. A Sustainable Development Goal for
694 Rio+ 20. *Policy Brief, May*.
- 695 Webb, R. H. (2002). Recovery of Severely Compacted Soils in the Mojave Desert,
696 California, USA. *Arid Land Research and Management*, 16(3), 291-305.
697 doi:<https://doi.org/10.1080/153249802760284829>
- 698 Wei, W., Chen, L., Fu, B., Huang, Z., Wu, D., & Gui, L. (2007). The effect of land
699 uses and rainfall regimes on runoff and soil erosion in the semi-arid loess hilly
700 area, China. *Journal of Hydrology*, 335(3), 247-258.
701 doi:<https://doi.org/10.1016/j.jhydrol.2006.11.016>
- 702 Weigelt, P., Steinbauer, M. J., Cabral, J. S., & Kreft, H. (2016). Late Quaternary
703 climate change shapes island biodiversity. *Nature*, 532, 99.
704 doi:<https://doi.org/10.1038/nature17443>
- 705 Whitford, W. G. (2002). *Ecology of desert systems*: Elsevier.
- 706 Yin, D., Roderick, M. L., Leech, G., Sun, F., & Huang, Y. (2014). The contribution of
707 reduction in evaporative cooling to higher surface air temperatures during
708 drought. *Geophysical Research Letters*, 41(22), 7891-7897.
709 doi:<https://doi.org/10.1002/2014GL062039>

710

711 **Supporting Information**

This article is protected by copyright. All rights reserved

712 Additional Supporting Information, including Figures S1-10, Method S1 and Tables
713 S1 and S2, may be found online in the supporting information tab for this article.

714

715 **Data availability**

716 Data in the support of these findings (Data S1) and the R code for the statistical
717 models conducted are available in figshare (DOI 10.6084/m9.figshare.7570925,
718 <https://figshare.com/s/4985715ce88482a9c460>).

719

720 **Table 1** Coefficients of the generalized least squares model fitted to assess the effect
721 of different predictor variables on ecosystem multifunctionality. This model included
722 a spatial correlation structure to account for the autocorrelation present within the 236
723 sites surveyed. We also removed the predictors with low power and the final model
724 had the lowest Akaike information criteria (see Methods section for details). The
725 predictor variables with significant explanatory power ($P < 0.05$) included desert
726 legacy, mean annual temperature (MAT) legacy, current MAT, soil sand content, and
727 site elevation (Elevation², square of elevation).

Predictor variables	Coefficients (mean ± standard error)	<i>P</i>-value
Intercept	1.591 ± 0.170	<0.001
Desert legacy	-0.295 ± 0.061	<0.001
MAT legacy	-0.085 ± 0.017	<0.001
Current MAT	-0.021 ± 0.006	<0.001
Soil sand content	-0.011 ± 0.001	<0.001
Elevation ²	0.001 ± 0.000	0.009

728

729 **Table 2** The total standardized effects (direct + indirect) of desert legacy, climate legacy, and current desert and climate on 12 individual
 730 ecosystem functions, based on the significant path coefficients ($P < 0.05$) of confirmatory path analyses. SOC, soil organic carbon; PEN, soil
 731 pentoses; iNDVI, annual integral of normalized difference vegetation index; HEX, soil hexoses; NIT, soil nitrate; DON, soil dissolved organic
 732 nitrogen; PRO, soil proteins; NTR, soil potential nitrogen transformation rate; AVP, soil available inorganic phosphorus; FOS, soil enzymatic
 733 activity of phosphatase; TP, soil total phosphorus; IOP, soil inorganic phosphorus; MAT, mean annual temperature; MAP, annual precipitation;
 734 Species, plant species richness; Sand, soil sand content; and site elevation (Elevation², square of elevation).

	SOC	iNDVI	PEN	HEX	NIT	DON	PRO	NTR	AVP	FOS	TP	IOP
Desert legacy	-0.21	-0.19	0	-0.33	0	0	0	0	0	-0.12	-0.19	0
MAT legacy	-0.19	-0.13	-0.37	-0.27	-0.12	0.43	-0.35	-0.1	0.12	-0.28	-0.39	0.08
MAP legacy	-0.01	-0.14	-0.33	0	0.35	0	0	0	0.2	-0.13	0.22	0.14
Current desert	0	0	0	0	0	0	0	0	0.19	-0.14	0	0
Current MAT	-0.62	0	-0.61	-0.18	-0.27	0.32	0	-0.36	-0.33	-0.64	-0.75	0.07
Current MAP	0.27	0.58	0	0.53	-0.03	0.07	-0.37	0.11	-0.34	0.46	0.14	-0.32
Species	0.16	0	0	0.1	0	0	0	0	0	0.09	0	0
Sand	-0.47	0	0	-0.16	-0.32	-0.16	0	-0.24	0	-0.34	-0.3	0.21
pH	0.31	0	0	0.2	0	0	0.24	0	0	0.28	0	0
pH ²	-0.34	0	0	-0.22	0	0	0	0	0	-0.31	0	0
Elevation	-0.09	0.48	-0.52	-0.05	-0.14	0.44	0.68	0	0	0	0	0
Elevation ²	0.23	-0.74	0	-0.08	-0.16	-0.07	-0.67	-0.32	0	-0.55	-0.14	0.1

736 **Figure captions**

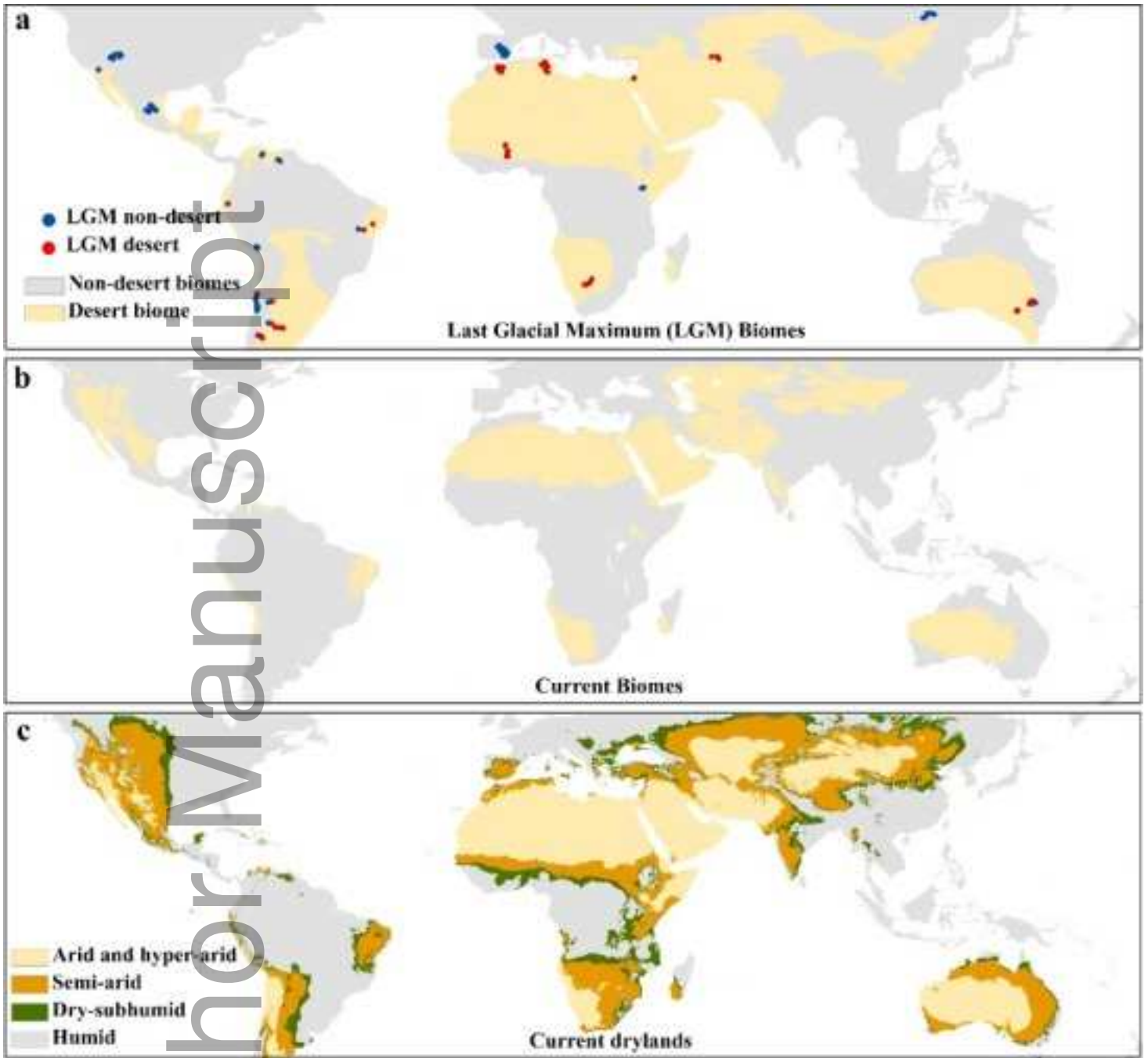
737 **Figure 1** Geographic locations of the 236 dryland sites surveyed and distribution of
738 global desert biomes and drylands. The desert biomes under the Last Glacial
739 Maximum **(a)** and current environmental conditions **(b)** were obtained from Ray &
740 Adams (2001) and Olson et al. (2001), respectively. The current extent of drylands, as
741 defined by the aridity index (AI, the ratio of precipitation to potential
742 evapotranspiration), is shown in panel **(c)** (source: Trabucco & Zomer, 2009).
743 Drylands include arid and hyper-arid ($AI < 0.2$), semi-arid ($0.2 \leq AI < 0.5$) and dry
744 sub-humid ($0.5 \leq AI < 0.65$) regions.

745

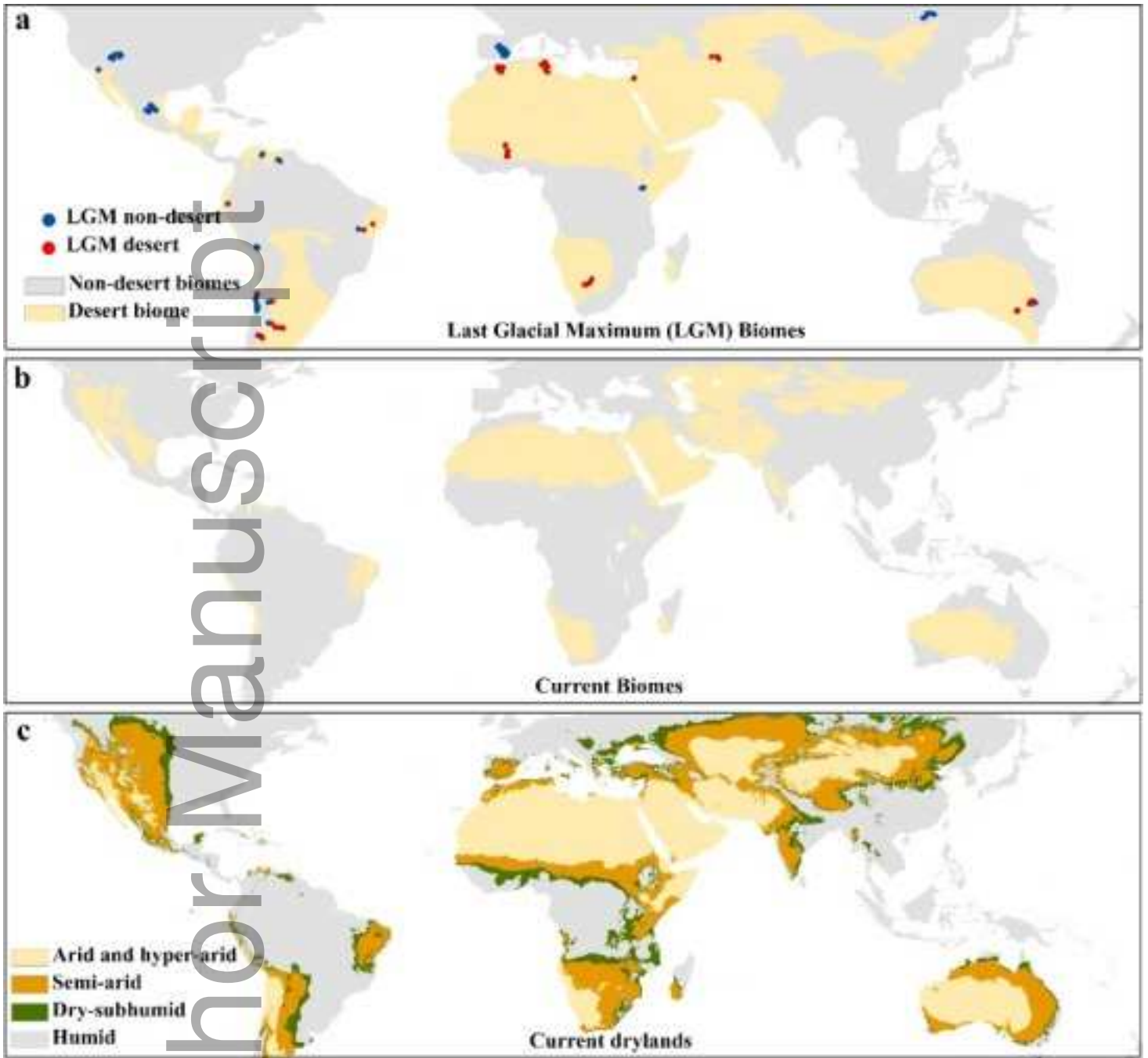
746 **Figure 2** The unique and shared proportions of variations in multifunctionality
747 explained by different predictors. We used variation partitioning analysis to calculate
748 the proportions of variations. Significance levels are as follows: *** $P < 0.001$, ** $P <$
749 0.01 . The significance of the shared variation could not be statistically tested. The
750 unexplained residual variance was 0.49.

751

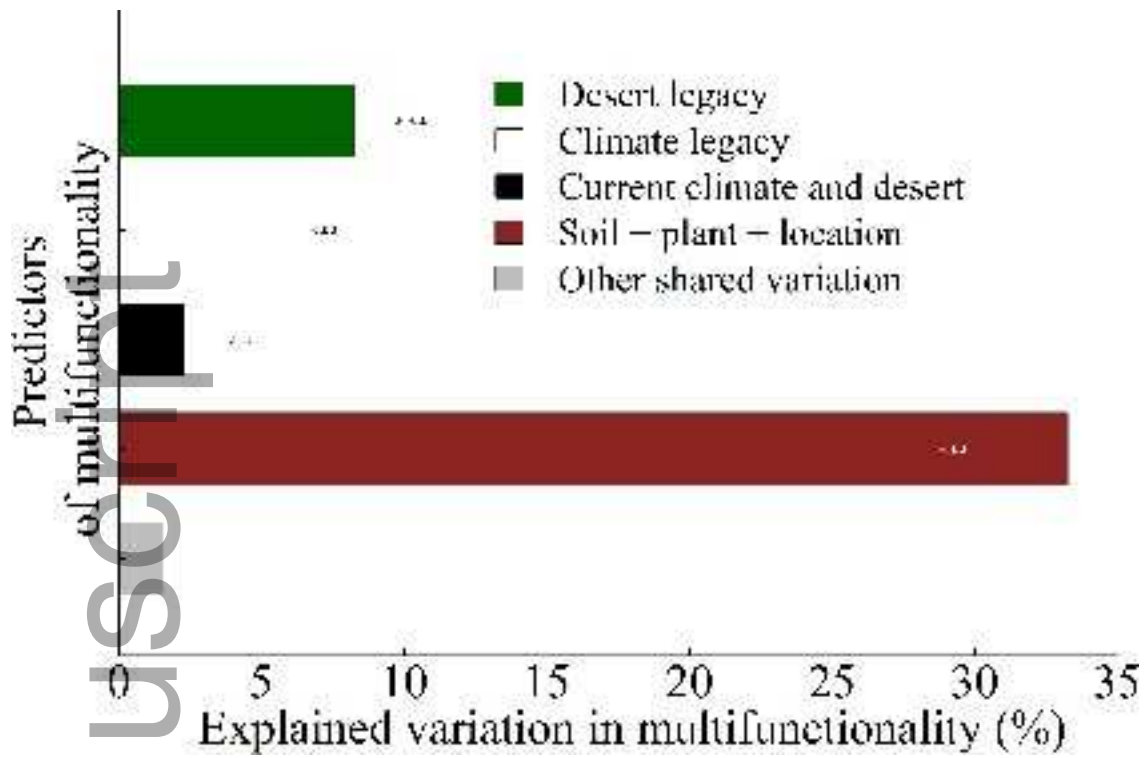
752 **Figure 3** Confirmatory path analysis (CPA) accounting for the direct and indirect
753 effects of environmental predictors on multifunctionality. **(a)** The significant path
754 coefficients, describing the strength and sign of the relationships among the variables,
755 are shown adjacent to the arrows (significance levels as follows: *** $P < 0.001$, ** P
756 < 0.01 , * $P < 0.05$). Paths of site elevation and slope were not included for simplicity,
757 since the main objective of this study was to evaluate the legacy effects of climate and
758 biome. MAT: mean annual temperature; MAP: annual precipitation; Soil sand: soil
759 sand content. The CPA conducted had a Fisher's $C = 5.57$, four degrees of freedom
760 and a P -value = 0.23, suggesting that it had a good fit to our data (Grace, 2006). **(b)**
761 Standardized total (direct + indirect) effects of desert and climate legacies, and of
762 current desert and climate on multifunctionality, based on CPA.



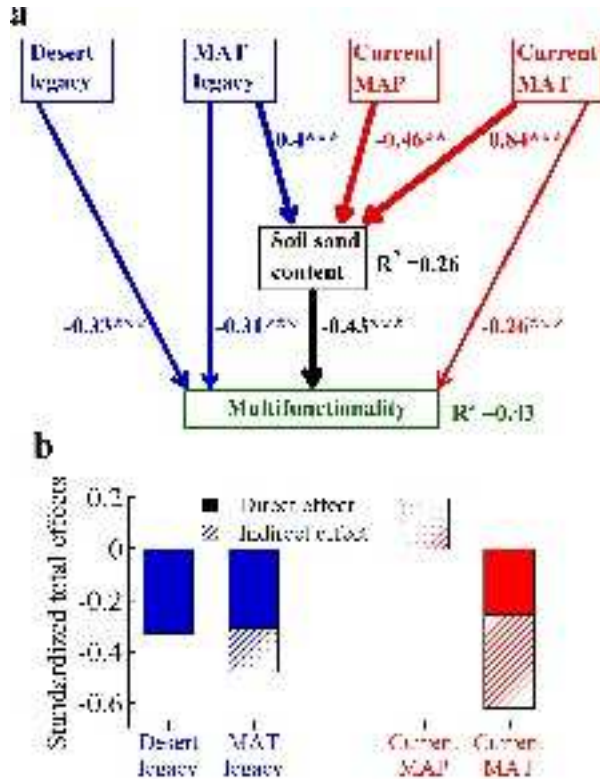
gcb_14631_f1.png



gcb_14631_f1.png



gcb_14631_f2.png



gcb_14631_f3.png